Polycyclic Aromatic Hydrocarbons

International Edition: DOI: 10.1002/anie.201913037
German Edition: DOI: 10.1002/ange.201913037

A Unified Mechanism on the Formation of Acenes, Helicenes, and Phenacenes in the Gas Phase

Long Zhao, Ralf I. Kaiser, Bo Xu, Utuq Ablikim, Musahid Ahmed,* Mikhail M. Evseev, Eugene K. Bashkirov, Valeriy N. Azyazov, and Alexander M. Mebel**

Abstract: *A unified low-temperature reaction mechanism on the formation of acenes, phenacenes, and helicenes—polycyclic aromatic hydrocarbons (PAHs) that are distinct via the linear, zigzag, and ortho-condensed arrangements of fused benzene rings—is revealed. This mechanism is mediated through a barrierless, vinylacetylene mediated gas-phase chemistry utilizing tetracene, [4]phenacene, and [4]helicene as benchmarks contesting established ideas that molecular mass growth processes to PAHs transpire at elevated temperatures. This mechanism opens up an isomer-selective route to aromatic structures involving submerged reaction barriers, resonantly stabilized free-radical intermediates, and systematic ring annulation potentially yielding molecular wires along with racemic mixtures of helicenes in deep space. Connecting helicene templates to the Origins of Life ultimately changes our hypothesis on interstellar carbon chemistry.*

Introduction

Tetracene (naphthacene; $C_{18}H_{12}$),[1] [4]phenacene (chrysene; $C_{18}H_{12}$),[2] and [4]helicene (benzo[*c*]phenanthrene; $C_{18}H_{12}$)[3] isolated nearly a century ago are the simplest representatives of three key classes of polycyclic aromatic hydrocarbons (PAHs)—acenes, phenacenes, and helicenes—structural isomers of aromatic systems differentiated by linear, zigzag, and *ortho*-condensed arrangements of fused benzene rings. These species received considerable attention as molecular tracers in untangling the underlying molecular mass growth processes leading to PAHs in combustion systems and in the interstellar medium (ISM) at the most fundamental, microscopic level (Scheme 1). Although the presence of PAHs[4] along with their methylated and hetero-

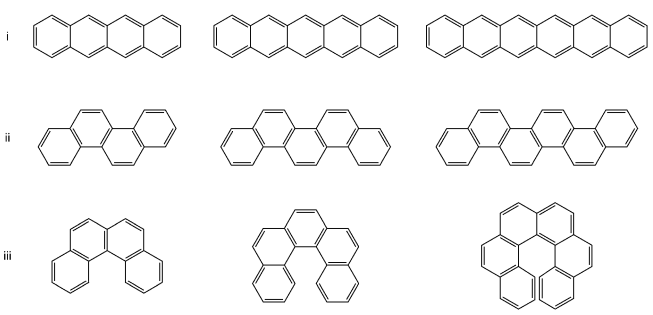

Scheme 1. Representatives of key classes of PAHs differing by the linear, zigzag, and *ortho*-condensed arrangements of fused benzene rings: acenes (i), phenacenes (ii), and helicenes (iii).

atom substituted counterparts[5] have been firmly established in carbonaceous chondrites, such as Allende and Murchison with PAHs possibly accounting for up to 20% of the cosmic carbon budget,[6] the underlying mechanisms to their formation beyond anthracene ($C_{14}H_{10}$) and phenanthrene ($C_{14}H_{10}$)[7] in deep space and in combustion systems have remained largely elusive.

Recent laser desorption–laser multiphoton ionization mass spectrometry (L^2MS) along with D/H and $^{13}C/^{12}C$ isotopic analyses of meteoritic PAHs revealed that these meteoritic PAHs are likely synthesized in circumstellar envelopes of carbon-rich Asymptotic Giant Branch Stars (AGB) and planetary nebulae as the descendants of AGB stars via extensive molecular mass growth processes.[4a,c,8] However, contemporary astrochemical models of PAH formation as derived from combustion chemistry reaction networks[9] predict time scales for the injection of PAHs from carbon stars into the interstellar medium of some 10^9 years, which is much longer than the predicted lifetimes of PAHs of only a few 10^8 years.[10] These models rely on the much discussed hydrogen-abstraction/acetylene-addition (HACA) mechanism, which involves repetitive sequences of atomic hydrogen abstractions from an aromatic hydrocarbon like benzene followed by consecutive addition of one or two acetylene molecule(s) prior to cyclization and aromatization.[11] Interstellar PAHs can be rapidly destroyed by photolysis,[12] galactic cosmic rays,[13] and interstellar shocks,[10]

[*] Dr. L. Zhao, Prof. R. I. Kaiser
Department of Chemistry
University of Hawaii at Manoa
Honolulu, HI 96822 (USA)
E-mail: ralfk@hawaii.edu
Dr. B. Xu, Dr. U. Ablikim, Dr. M. Ahmed
Chemical Sciences Division
Lawrence Berkeley National Laboratory
Berkeley, CA 94720 (USA)
E-mail: mahmed@lbl.gov
M. M. Evseev, Prof. E. K. Bashkirov, Prof. V. N. Azyazov, Prof. A. M. Mebel
Samara National Research University
Samara 443086 (Russia)
Prof. A. M. Mebel
Department of Chemistry and Biochemistry
Florida International University
Miami, FL 33199 (USA)
E-mail: mebela@fiu.edu
Supporting information and the ORCID identification number(s) for the author(s) of this article can be found under: https://doi.org/10.1002/anie.201913037.

but—along with their derivatives—they are still present as evidenced from the diffuse interstellar bands (DIBs)[14]—discrete absorption features overlaid on the interstellar extinction curve from the blue part of the visible (400 nm) to the near-infrared (1.2 mm)—and from unidentified infrared (UIR) emission bands[15] in the 3–14 mm wavelength range. Thus, the spectroscopic observation of PAHs infers a critical, hitherto unexplained route to their rapid chemical growth in the cold interstellar medium at temperatures down to 10 K.

Herein, we reveal an isomer-selective, versatile reaction mechanism involving vinylacetylene mediated gas phase formation of acenes, helicenes, and phenacenes with the simplest 18-π-electron tetracene, [4]phenacene, and [4]helicene isomers acting as critical benchmarks. In strong contrast to the aforementioned routes to PAHs synthesis involving HACA, our mechanistical studies of the elementary reactions of distinct anthracenyl and phenanthrenyl radicals ($[C_{14}H_9]^{\bullet}$; 177 amu) with vinylacetylene (C_4H_4; 52 amu) display barrierless pathways via the initial formation of a long-range van-der-Waals complexes in the entrance channels followed by isomerization through addition of the aromatic radical involving a submerged barrier leading to resonantly stabilized free $[C_{18}H_{13}]^{\bullet}$ radicals (RSFRs) [Equation (1)]. The latter

$$[C_{14}H_9]^{\bullet} + C_4H_4 \rightarrow [C_{18}H_{13}]^{\bullet} \rightarrow C_{18}H_{12} + H^{\bullet} \quad (1)$$

undergo hydrogen migration and ring closure followed by aromatization through atomic hydrogen loss yielding distinct $C_{18}H_{12}$ isomers through targeted, stepwise ring expansion involving free radical reaction intermediates. This pathway represents a versatile reaction mechanism to synthesize acenes, helicenes, and phenacenes in low temperature interstellar environments down to 10 K through elementary gas phase reactions of aryl radicals with vinylacetylene. Considering the low temperature, bimolecular gas phase reactions have to be exoergic and all transition states involved shall be lower than the energy of the separated reactants. Since these requirements are fulfilled, the proposed pathway provides a hitherto ignored low temperature route to complex PAHs via ring annulation. Interstellar PAHs are rapidly destroyed in the interstellar medium by photolysis, cosmic rays, and interstellar shocks leading to life times of only a few 10^8 years.[10] This time scale is much shorter than the time scale for injection of PAHs synthesized in carbon-rich outflows of AGB stars of some 10^9 years.[10] Therefore, the presence of PAH-like material in the interstellar medium suggests that a critical synthetic pathway to PAHs at low temperatures is missing. The mechanisms elucidated here might fill the gap and can provide a unique route to PAHs at temperatures as low as 10 K. These mechanisms are of interest in organic chemistry and can be linked to material sciences as they provide insight into reactivity, bond-breaking processes, and synthesis of extended π-conjugated systems involving acyclic precursors (vinylacetylene) with extensive applications as building blocks for molecular wires,[16] carbon nanotubes[17] and graphene[18] along with molecular organic semiconductors for organic field effect transistors[19] and organic light emitting diodes.[20]

Briefly, a high-temperature chemical reactor was utilized to investigate the reaction of distinct anthracenyl and phenanthrenyl radicals ($[C_{14}H_9]^{\bullet}$) with vinylacetylene (C_4H_4). This reactor[7,9] consists of a heated silicon carbide (SiC) tube and is incorporated within the source chamber of a molecular beam machine equipped with a Wiley–McLaren reflectron time-of-flight mass spectrometer (Re-TOF-MS) (Figure 1). To generate the radical reactants, thermally labile brominated precursor molecules were pyrolyzed in situ via cleavage of a weak carbon–bromine bond. These precursors

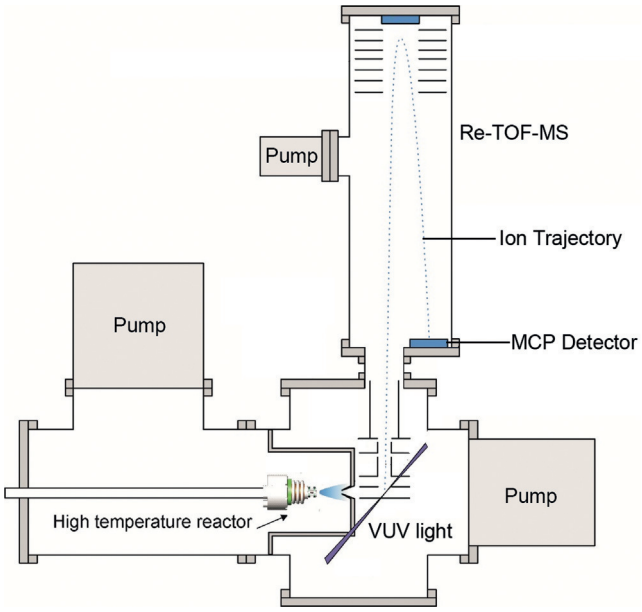

Figure 1. Schematic diagram of the high-temperature reactor along with the molecular beam sampling reflectron time-of-flight mass spectrometer.[21]

were 2- and 3-bromophenanthrene along with 1- and 2-bromoanthracene ($C_{14}H_9Br$) seeded in separate experiments in vinylacetylene/helium. The temperature of the reactor was 1400 ± 10 K. At this temperature, each brominated precursor dissociates to the corresponding radical plus atomic bromine in situ followed by reaction of the radical with vinylacetylene. The reaction products were expanded, passed through a skimmer downstream the reactor, and entered the main chamber, which houses the Re-TOF-MS. Tunable vacuum ultraviolet (VUV) light from the Advanced Light Source crossed the neutral molecular beam downstream of the skimmer in the extraction region of the Re-TOF-MS. A mass spectrum was collected by measuring the arrival time of the ions, as a function of mass-to-charge (m/z) ratios. Finally, photoionization efficiency (PIE) curves reporting the ion counts of well-defined m/z ratios versus the VUV energy were recorded by integrating the ion signal at mass-to-charges of interest and normalizing it to the photon flux. VUV single photon ionization represents a fragment-free ionization technique and is dubbed as a *s*oft ionization method compared to the harsher conditions of electron impact ionization leading often to excessive fragmentation of the parent ion (Supporting Information).

Results and Discussion

Mass Spectra

As a very first step, we analyze the mass spectra of each system qualitatively and extract the molecular formulae of the reaction products. Representative mass spectra recorded at a photoionization energy of 9.50 eV are displayed in Figure 2 for the reactions of 1- and 2-bromoanthracenyl (Figures 2 b,d) and 2- and 3-bromophenanthrenyl (Figures 2 f,h) with vinylacetylene. We also conducted "blank" experiments by replacing the vinylacetylene reactant with non-reactive helium carrier gas (Figures 2 a,c,e,g) to guarantee that the newly emerging products (Figures 2 b,d,f,h) are the result of the reaction of the radicals with vinylacetylene. A detailed inspection of these data reveals the formation of molecules with the molecular formulae $C_{16}H_{10}$ (202 amu) and $C_{18}H_{12}$ (228 amu) along with the ^{13}C isotopologues at m/z 203 and 229 in all systems. These ion counts are clearly absent in the control experiments suggesting that molecules detected via m/z 202, 203, 228, and 229 represent reaction products in all $C_{14}H_9$–C_4H_4 systems. Considering the molecular weight of the reactants and the products, the $C_{18}H_{12}$ isomers along with atomic hydrogen are the result of the reaction of the aromatic radicals with vinylacetylene through the reaction in Eq. (1). The signal for $C_{16}H_{10}$ (202 amu) can be attributed to the reaction of the anthracenyl/phenanthrenyl radicals with acetylene (C_2H_2; 26 amu) and might be linked to the formation of ethynyl-substituted anthracenes and phenanthrenes (Figures S1–S4 in the Supporting Information). The

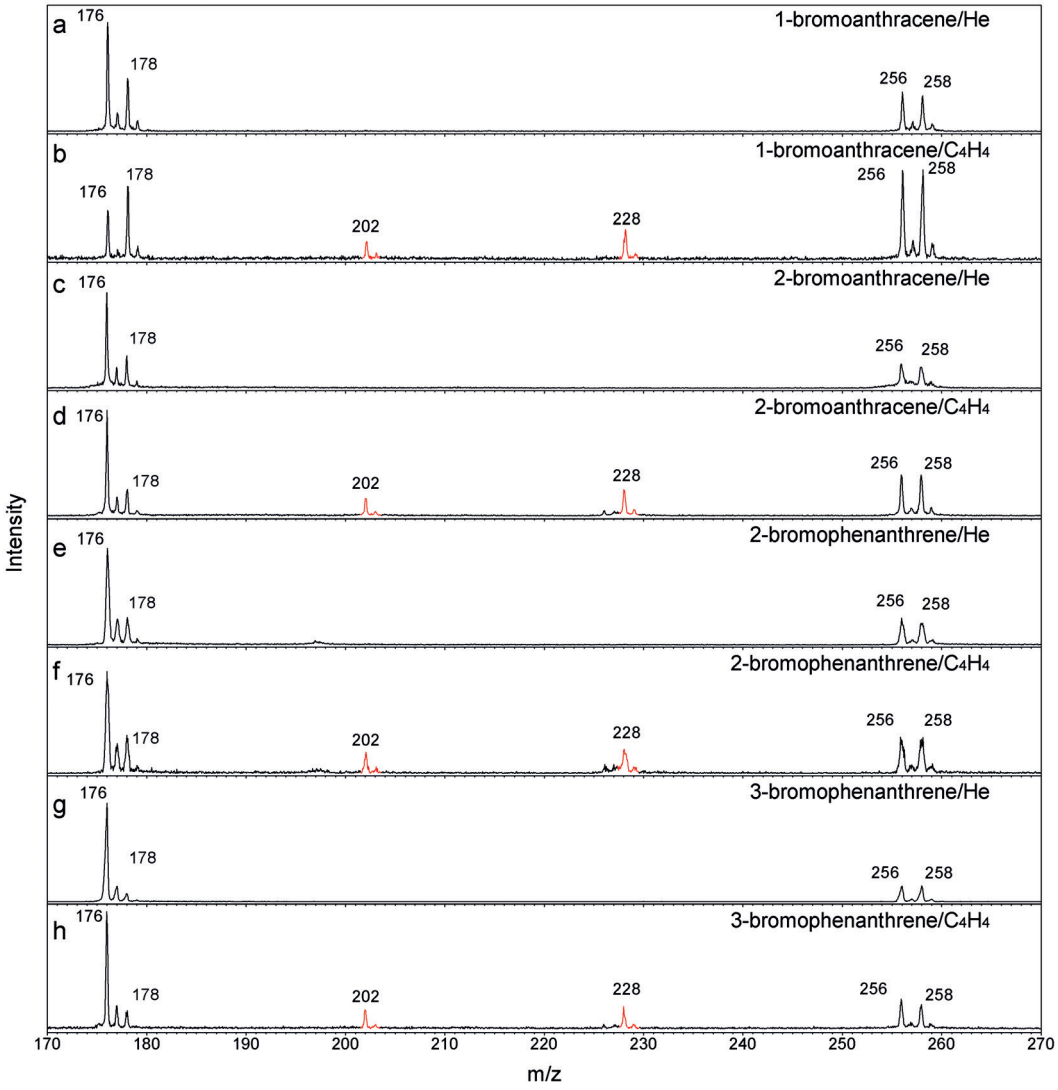

Figure 2. Mass spectra recorded at a photoionization energy of 9.50 eV. a) 1-bromoanthracene–helium, b) 1-bromoanthracene–vinylacetylene, c) 2-bromoanthracene–helium, d) 2-bromoanthracene–vinylacetylene, e) 2-bromophenanthrene–helium, f) 2-bromophenanthrene–vinylacetylene, g) 3-bromophenanthrene–helium, and h) 3-bromophenanthrene—vinylacetylene systems. The ion peaks of the newly formed $C_{16}H_{10}$ (m/z 202) and $C_{18}H_{12}$ (m/z 228) species along with the ^{13}C-substituted counterparts (m/z 203 and 229) are highlighted in red.

ion counts at m/z of 259 ($C_{13}{}^{13}CH_9{}^{81}Br^+$), 258 ($C_{14}H_9{}^{81}Br^+$), 257 ($C_{13}{}^{13}CH_9{}^{79}Br^+$), 256 ($C_{14}H_9{}^{79}Br^+$), 179 ($C_{13}{}^{13}CH_{10}{}^+$), 178 ($C_{14}H_{10}{}^+$), 177 ($C_{14}H_9{}^+/C_{14}{}^{13}CH_8{}^+$), and 176 ($C_{14}H_8{}^+$) are detectable in the control experiments as well and hence cannot be associated with the reaction of anthracenyl/phenanthrenyl radicals with vinylacetylene (Figures S1–S4).

Photoionization Efficiency (PIE) Curves

The analysis of the mass spectra provided compelling evidence that $C_{18}H_{12}$ isomer(s) are formed via the reaction of anthracenyl/phenanthrenyl radicals with vinylacetylene. The primary goal of this study is, however, to elucidate which $C_{18}H_{12}$ isomer(s) is/are formed. This requires a detailed inspection of the corresponding photoionization efficiency (PIE) curves at m/z 228 ($C_{18}H_{12}{}^+$). Here, each PIE curve reports the number of ions detected at a well-defined m/z ratio such as m/z 228 as a function of the photon energy from 7.20 eV to 10.00 eV (Figure 3). It is important to highlight that the PIE curves of distinct $C_{18}H_{12}$ isomers are very different and hence unique. This is evident from distinct PIE curves of the $C_{18}H_{12}$ isomers—tetracene (naphthacene), [4]phenacene (chrysene), [4]helicene (benzo[*c*]phenanthrene), benz[*a*]anthracene, triphenylene—recorded in separate calibration experiments (Figure S5). Therefore, the PIE calibration curves can be utilized to discriminate between multiple $C_{18}H_{12}$ isomers. More than one $C_{18}H_{12}$ isomer might be formed in each reaction investigated, and therefore each experimental PIE curve at m/z 228 represents the sum, that is, a linear combination, of the calibrated PIE curves of the individual isomers. Consequently, the experimental PIE curves have to be fit with a linear combination of the PIE calibration curves of distinct isomers.

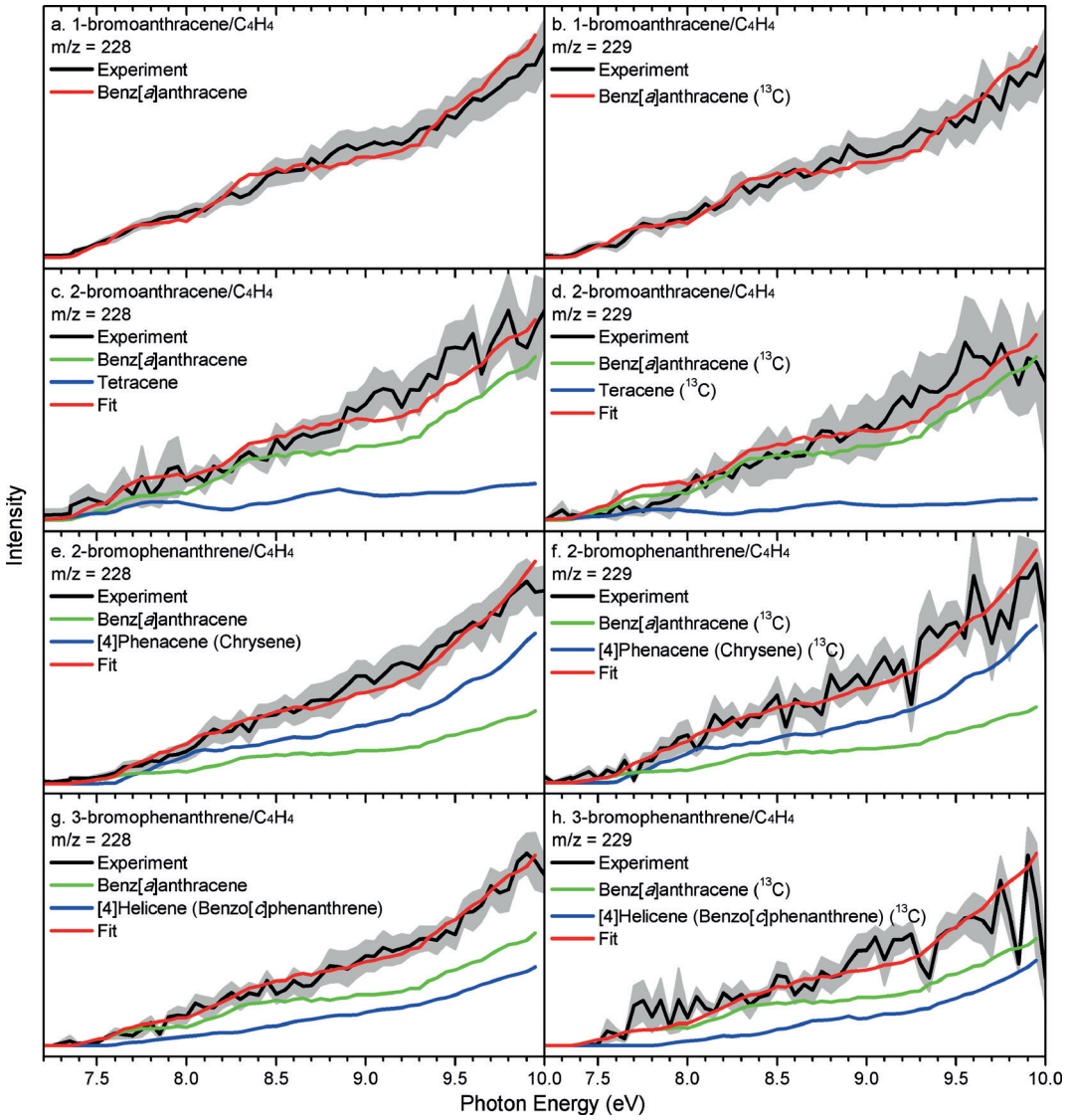

Figure 3. Photoionization efficiency (PIE) curves for m/z 228 and 229. a),b) 1-bromoanthracene–vinylacetylene; c),d) 2-bromoanthracene–vinylacetylene; e),f) 2-bromophenanthrene–vinylacetylene; g),h) 3-bromophenanthrene–vinylacetylene. Black lines: experimentally derived PIE curves; colored lines: reference PIE curves. In case of multiple contributions to one PIE curve, the red line shows the overall fit. The overall error bars consist of two parts: ±10% based on the accuracy of the photodiode and a 1σ error of the PIE curve averaged over the individual scans.

Discussion

In the 1-anthracenyl-vinylacetylene system, the experimental PIE curve can be fit within the error limits with a single reference PIE curve of benz[*a*]anthracene (Figures 3a,b). Both PIE curves depict an onset of the ion signal at 7.35 ± 0.05 eV, which agrees nicely with the adiabatic ionization energy of benz[*a*]anthracene of 7.41 ± 0.02 eV.[22] The remaining three systems of 2-anthracenyl, 2-phenanthrenyl, and 3-phenanthrenyl with vinylacetylene require a linear combination of two reference curves of benz[*a*]anthracene/tetracene, [4]phenacene/benz[*a*]anthracene, and [4]helicene/benz[*a*]anthracene, respectively (Figures 3c–h). Corresponding PIE curves of *m*/*z* 229 ($^{13}CC_{17}H_{12}^{+}$) match these findings and reveal that ion signal at *m*/*z* 229 originates solely from the aforementioned ^{13}C-isotoplogue PAHs. Therefore, we can conclude that our studies provide compelling evidence on the formation of four distinct $C_{18}H_{12}$ isomers of PAHs with benz[*a*]anthracene being identified in all four systems; tetracene, [4]phenacene, and [4]helicene represent distinct reaction products (Figures 4–7).

The experimental data provide persuasive evidence on the formation of the simplest representatives of three key classes of PAHs, that is, acenes, phenacenes, and helicenes, formed through the elementary reactions of anthracenyl and phenanthrenyl radicals with vinylacetylene in the gas phase. These representatives are: tetracene, [4]phenacene, and [4]helicene, respectively, along with benz[*a*]anthracene. Our goal is not only to identify the PAH isomers formed, but also to elucidate the underlying reaction mechanisms. In case of polyatomic complex systems, it is useful to combine the experimental results with electronic structure calculations to untangle the synthetic routes (Figures 4–7). Our computations reveal that for each reaction, the radical reactant approaches the vinylacetylene molecule resulting in the formation of weakly stabilized van-der-Waals complex (**1.1**–**1.4**, Figures 4–7) bound by 8–12 kJ mol^{-1} with rather long carbon–carbon distances between 413 pm and 526 pm. The complexes isomerize via addition of the radical center to the terminal sp^2 carbon of the vinylic group in vinylacetylene resulting in the formation of distinct $C_{18}H_{13}$ intermediates (**2.1**–**2.4**, Figures 4–7). These processes involve barriers located 4 to 9 kJ mol^{-1} *above* the van-der-Waals complexes, but below the energy of the separated reactants. In this case, a barrier to addition does exist, but since the transition state is lower in energy than the reactants, this barrier is submerged with respect to the reactants and hence is called a submerged barrier. Hereafter, these intermediates isomerize via hydrogen shifts from the aromatic ring from the carbon atom adjacent to the former radical center to the vinylacetylene moiety forming a -CH_2-C**H**H-CCH side chain with the migrated hydrogen atom denoted in bold. Eventually, the

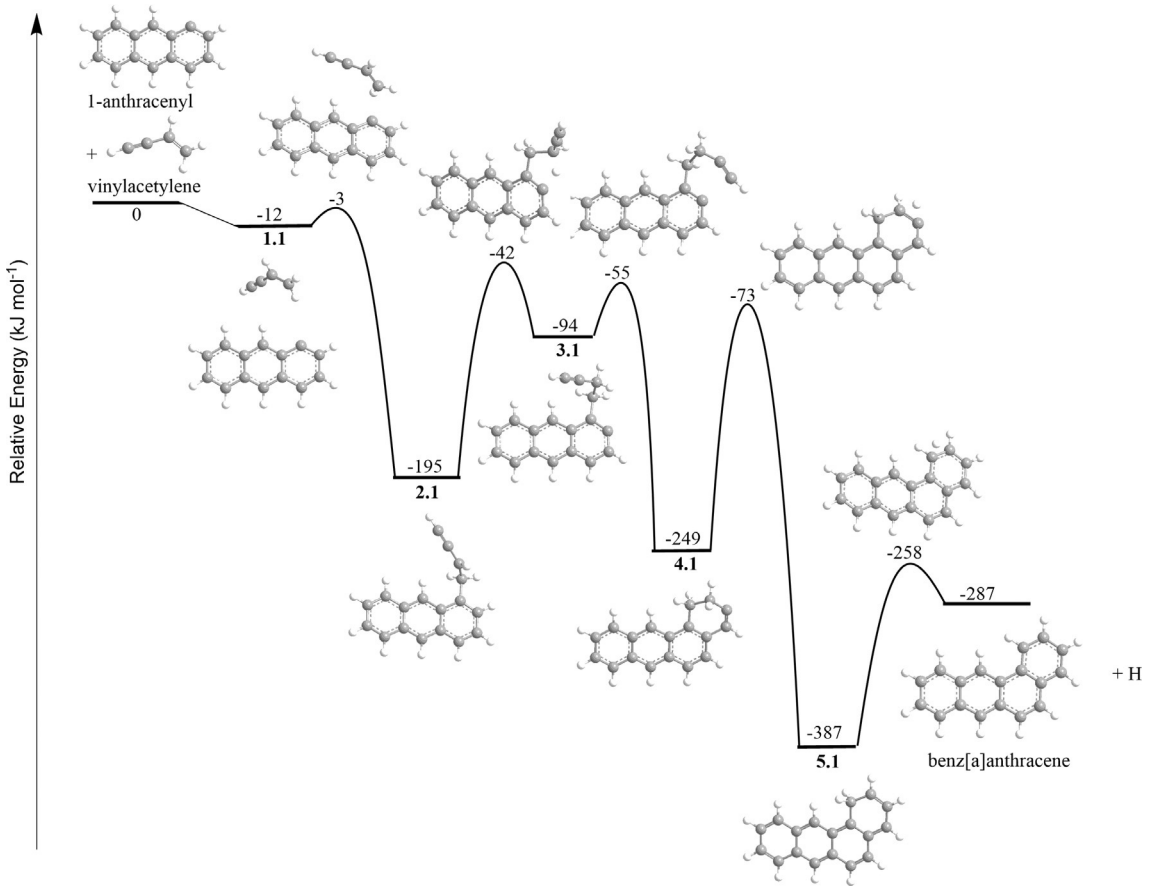

Figure 4. Potential energy surfaces (PESs) of 1-anthracenyl leading to the formation of benz[*a*]anthracene. Relative energies with respect to the reactants are given in kJ mol^{-1}.

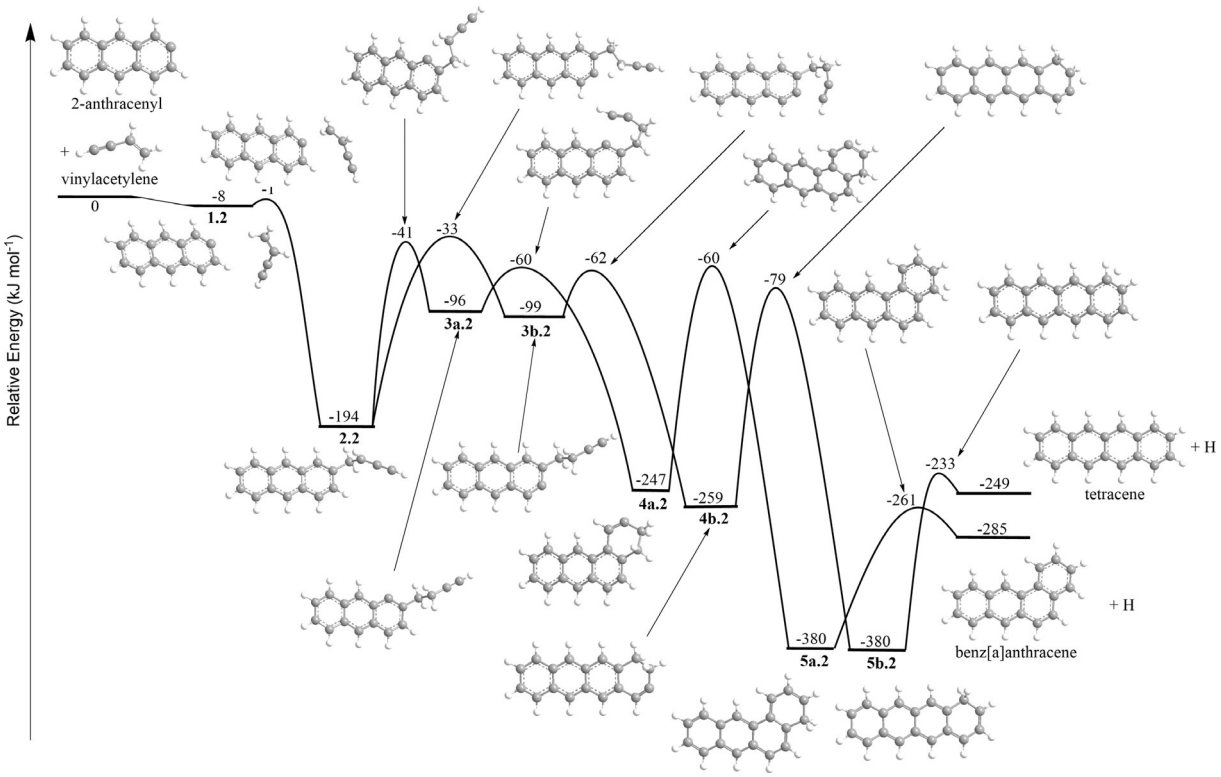

Figure 5. Potential energy surfaces (PESs) of 2-anthracenyl leading to the formation of benz[*a*]anthracene and tetracene. Relative energies with respect to the reactants are given in kJ mol^{-1}.

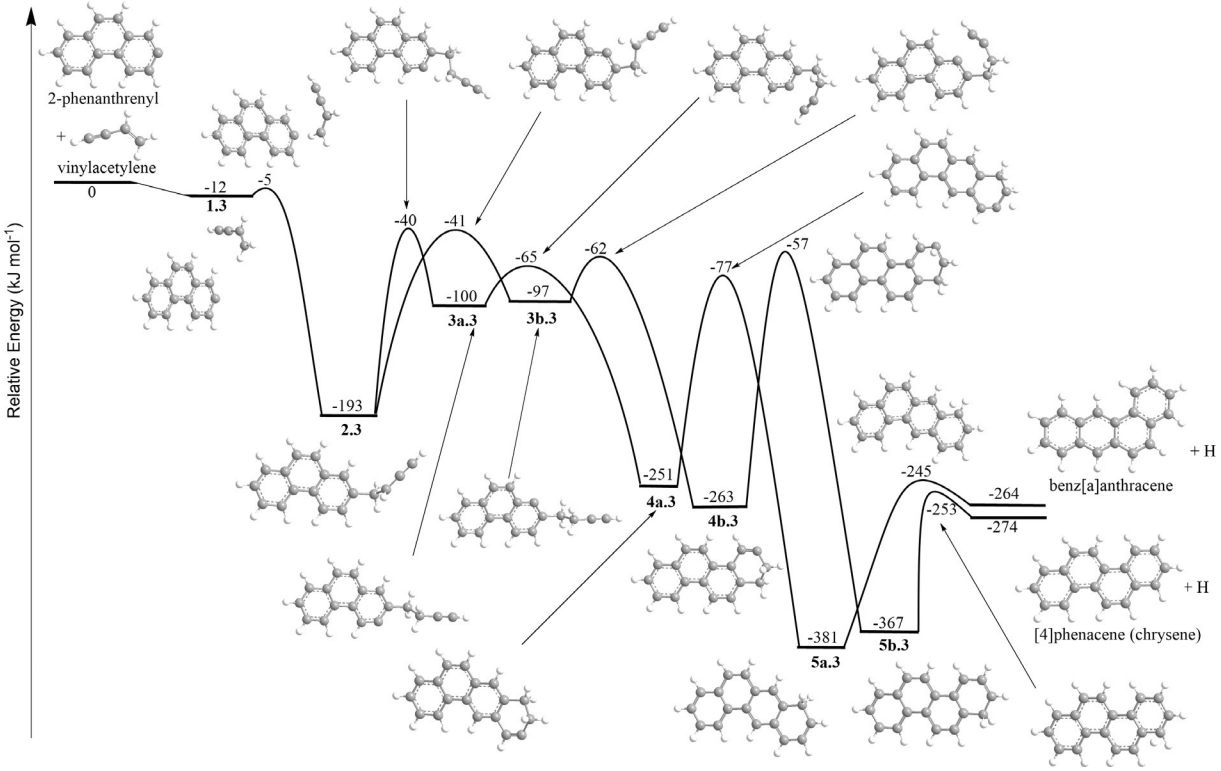

Figure 6. Potential energy surfaces (PESs) of 2-phenanthrenyl leading to the formation of benz[*a*]anthracene and [4]phenacene. Relative energies with respect to the reactants are given in kJ mol^{-1}.

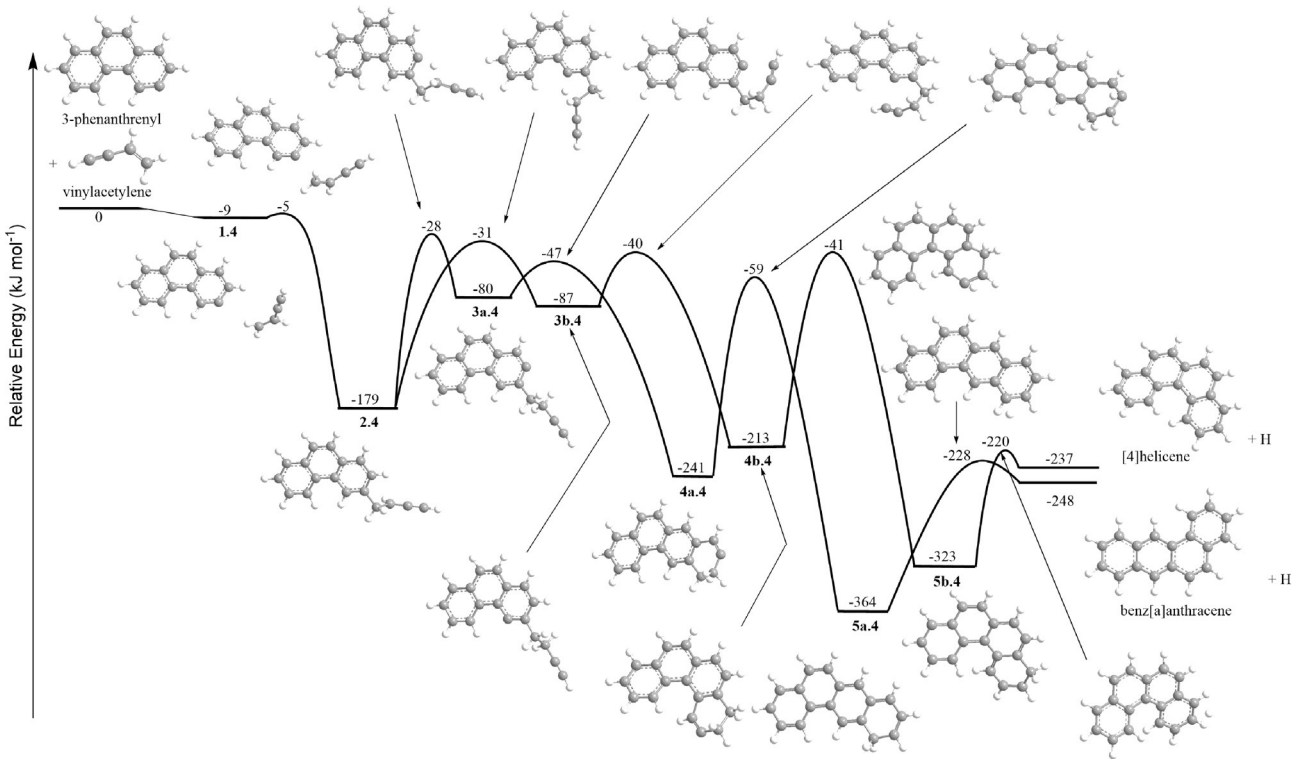

Figure 7. Potential energy surfaces (PESs) of 3-phenanthrenyl leading to the formation of benz[*a*]anthracene and [4]helicene. Relative energies with respect to the reactants are given in kJ mol^{-1}.

newly formed intermediates (**3.1**–**3.4**, Figures 4–7) undergo facile ring closure yielding PAH-type radicals which carry four six-membered rings (**4.1**–**4.4**; Figures 4–7). A comparison of the molecular structures of these intermediates with the detected reaction products benz[*a*]anthracene (Figure 4), tetracene/benz[*a*] anthracene (Figure 5), [4]phenacene/benz-[*a*]anthracene (Figure 6), and [4]helicene/benz[*a*]anthracene (Figure 7) suggests that in each radical intermediate, a hydrogen atom has to migrate from the CH_2 moiety of the newly formed ring to the neighboring bare carbon atom forming intermediates **5.1**–**5.4** (Figures 4–7). These intermediates eject atomic hydrogen accompanied by aromatization and formation of the closed shell PAH. The overall reactions are exoergic and all transition states are below the energy of the separated reactants. Benz[*a*]anthracene is formed in all systems, whereas tetracene, [4]phenacene, and [4]helicene are unique to the reactions of 2-anthracenyl, 2-, and 3-phenanthrenyl with vinylacetylene, respectively.

Conclusion

In conclusion, our combined experimental and computational study provides compelling evidence of an isomer-selective, unified mechanism to the simplest 18-π-aromatic acenes, phenacenes, and helicenes—tetracene, [4]phenacene, and [4]helicene—via vinylacetylene mediated gas phase reactions involving ring annulation of anthracenyl and phenanthrenyl radicals. These de facto barrierless routes are initiated through the formation of long-range van der Waals complexes, which can isomerize through addition of the radical reactant via transition states located below the energy of the separated reactants (submerged barrier). This submerged barrier represents a crucial prerequisite for a bimolecular reaction to proceed at low temperatures since any transition state located above the energy of the separated reactants cannot be overcome at low temperatures of 10 K. Since all reactions investigated are barrierless and exoergic, these elementary reactions may also contribute to the formation of PAHs in cold molecular clouds such as Taurus Molecular Cloud −1 (TMC-1) at temperatures as low as 10 K thus supplying a hitherto elusive low temperature molecular mass growth process to complex PAHs carrying four six-membered rings as detected along with benz[*a*]anthracene in carbonaceous chondrites, such as Murchison, Orgueil, and A-881458.[23] Here, the hydrogen abstraction—vinylacetylene addition (HAVA) pathway signifies a versatile reaction mechanism to generate even more complex acenes, helicenes, and phenacenes through barrierless, stepwise ring expansion via elementary gas phase reactions of an aryl radical, which can be formed inside molecular clouds from the corresponding aromatic precursor via photolysis by the internal ultraviolet field, with vinylacetylene. In circumstellar envelopes of carbon stars with temperatures of up to a few 1000 K and even in combustion flames, molecular mass growth processes could also be triggered by hydrogen abstraction from phenanthrene and anthracene followed by formation of tetracene, [4]phenacene, and/or [4]helicene as identified as products of incomplete combustion of coal,[24] wood,[25] and (bio)diesel.[26] This proposes HAVA as a facile key mechanism propelling

molecular mass growth processes of PAHs via de facto barrier-less, successive ring expansions involving elementary reactions of aryl radical with vinylacetylene as a molecular building block.

In cold molecular clouds such as the TMC-1, these processes may lead ultimately to molecular wires[16] and possibly racemic mixtures of helicenes depicting non-superimposable, clockwise and counterclockwise helices.[27] Should a preferential destruction of the minus (M) and plus (P) enantiomer, such as via photodissociation through circularly polarized light, exist, the resulting enantiomeric excess might be incorporated into carbonaceous grains, which can then become coated with nanometer thick icy layers of water (H_2O), ammonia (NH_3), methane (CH_4), carbon monoxide (CO), carbon dioxide (CO_2), and methanol (CH_3OH) in cold molecular clouds. Upon interaction of those ices with ionizing radiation, the grains might transmit their enantiomer excess to the newly formed complex organic molecules (COMs)—among them biorelevant molecules such as amino acids,[28] dipeptides,[29] and even carbon hydrates[30] thus connecting helicene templates to the Origins of Life ultimately changing our hypothesis on the interstellar carbon chemistry and the progression of carbonaceous matter in the universe on the most fundamental level.

Acknowledgements

This work was supported by the US Department of Energy, Basic Energy Sciences DE-FG02-03ER15411 (experimental studies) and DE-FG02-04ER15570 (computational studies) to the University of Hawaii and Florida International University, respectively. U.A., B.X., and M.A. are supported by the Director, Office of Science, Office of Basic Energy Sciences, of the U.S. Department of Energy under Contract No. DE-AC02-05CH11231, through the Gas Phase Chemical Physics program of the Chemical Sciences Division. The ALS is supported under the same contract. Ab initio calculations of the $C_{18}H_{13}$ PES relevant to the reactions of anthracenyl and phenanthrenyl radicals with vinylacetylene at Samara University were supported by the Ministry of Science and Higher Education of the Russian Federation under Grant No. 14.Y26.31.0020.

Conflict of interest

The authors declare no conflict of interest.

Keywords: gas-phase chemistry · hydrogen abstraction/vinylacetylene addition (HAVA) · interstellar medium · mass spectrometry · polycyclic aromatic hydrocarbons (PAHs)

How to cite: *Angew. Chem. Int. Ed.* **2020**, *59*, 4051 – 4058
Angew. Chem. **2020**, *132*, 4080 – 4087

[1] P. Valori, C. Melchiorri, A. Grella, G. Alimenti, *Nuovi Ann. Ig. Microbiol.* **1966**, *17*, 311.
[2] E. Oehler, *Angew. Chem.* **1899**, *12*, 561.
[3] R. Weitzenböck, A. Klingler, *Monatsh. Chem.* **1918**, *39*, 315.
[4] a) A. G. G. M. Tielens, *Annu. Rev. Astron. Astrophys.* **2008**, *46*, 289; b) A. Tielens, L. J. Allamandola in *Physics and Chemistry at Low Temperatures* (Ed.: Khriachtchev), Pan Stanford Publishing, Singapore, **2011**, pp. 341 – 380; c) A. G. G. M. Tielens, *Rev. Mod. Phys.* **2013**, *85*, 1021.
[5] L. J. Allamandola, *EAS Publ. Ser.* **2011**, *46*, 305.
[6] R. Zenobi, J. M. Philippoz, R. N. Zare, M. R. Wing, J. L. Bada, K. Marti, *Geochim. Cosmochim. Acta* **1992**, *56*, 2899.
[7] L. Zhao, R. I. Kaiser, B. Xu, U. Ablikim, M. Ahmed, M. M. Evseev, E. K. Bashkirov, V. N. Azyazov, A. M. Mebel, *Nat. Astron.* **2018**, *2*, 973.
[8] a) H. Naraoka, A. Shimoyama, K. Harada, *Earth Planet. Sci. Lett.* **2000**, *184*, 1; b) H. Naraoka, A. Shimoyama, K. Harada, *Mineral. Mag.* **1998**, *62A*, 1056.
[9] a) T. Yang, R. I. Kaiser, T. P. Troy, B. Xu, O. Kostko, M. Ahmed, A. M. Mebel, M. V. Zagidullin, V. N. Azyazov, *Angew. Chem. Int. Ed.* **2017**, *56*, 4515; *Angew. Chem.* **2017**, *129*, 4586; b) D. S. N. Parker, R. I. Kaiser, B. Bandyopadhyay, O. Kostko, T. P. Troy, M. Ahmed, *Angew. Chem. Int. Ed.* **2015**, *54*, 5421; *Angew. Chem.* **2015**, *127*, 5511.
[10] E. Micelotta, A. Jones, A. Tielens, *Astron. Astrophys.* **2010**, *510*, A36.
[11] a) M. Frenklach, E. D. Feigelson, *Astrophys. J.* **1989**, *341*, 372; b) M. Frenklach, *Phys. Chem. Chem. Phys.* **2002**, *4*, 2028.
[12] J. N. Grossman, A. P. Stern, M. L. Kirich, T. F. Kahan, *Atmos. Environ.* **2016**, *128*, 158.
[13] A. Jones, J. Nuth, *Astron. Astrophys.* **2011**, *530*, A44.
[14] W. Duley, *Faraday Discuss.* **2006**, *133*, 415.
[15] A. M. Ricks, G. E. Douberly, M. A. Duncan, *Astrophys. J.* **2009**, *702*, 301.
[16] D. Walter, D. Neuhauser, R. Baer, *Chem. Phys.* **2004**, *299*, 139.
[17] K. Itami, *Pure Appl. Chem.* **2012**, *84*, 907.
[18] D.-I. Son, W.-K. Choi in *Nanomaterials, Polymers and Devices* (Ed.: E. S. Kong), Wiley, Hoboken, **2015**, pp. 141 – 194.
[19] Y. Wang, S. Qiu, S. Xie, L. Zhou, Y. Hong, J. Chang, J. Wu, Z. Zeng, *J. Am. Chem. Soc.* **2019**, *141*, 2169.
[20] M. M. Islam, Z. Hu, Q. Wang, C. Redshaw, X. Feng, *Mater. Chem. Front.* **2019**, *3*, 762.
[21] L. Zhao, et al., *Phys. Chem. Chem. Phys.* **2017**, *19*, 15780.
[22] W. Schmidt, *J. Chem. Phys.* **1977**, *66*, 828.
[23] M. A. Sephton, G. D. Love, W. Meredith, C. E. Snape, C.-G. Sun, J. S. Watson, *Planet. Space Sci.* **2005**, *53*, 1280.
[24] M. Kaiho, Y. Kodera, O. Yamada, *Fuel* **2019**, *237*, 536.
[25] C. Achten, F. T. Beer, C. Stader, S. G. Brinkhaus, *Environ. Forensics* **2015**, *16*, 42.
[26] B. L. Valle-Hernández, O. Amador-Muñoz, A. Jazcilevich-Diamant, A. E. Hernández-López, R. Villalobos-Pietrini, R. González-Oropeza, *Combust. Sci. Technol.* **2013**, *185*, 420.
[27] R. S. Cahn, C. Ingold, V. Prelog, *Angew. Chem. Int. Ed. Engl.* **1966**, *5*, 385; *Angew. Chem.* **1966**, *78*, 413.
[28] M. Förstel, A. Bergantini, P. Maksyutenko, S. Góbi, R. I. Kaiser, *Astrophys. J.* **2017**, *845*, 83.
[29] R. Kaiser, A. Stockton, Y. Kim, E. Jensen, R. Mathies, *Astrophys. J.* **2013**, *765*, 111.
[30] C. Meinert, I. Myrgorodska, P. De Marcellus, T. Buhse, L. Nahon, S. V. Hoffmann, L. L. S. d'Hendecourt, U. J. Meierhenrich, *Science* **2016**, *352*, 208.

Manuscript received: October 11, 2019
Accepted manuscript online: December 23, 2019
Version of record online: January 23, 2020

